

# The energy dependence of exclusive heavy vector meson photoproduction cross-sections and NLO BFKL evolution

Martin Hentschinski and Ricardo Rangel Ramírez

Departamento de Actuaría, Física y Matemáticas, Universidad de las Américas Puebla,  
Santa Catarina Martir, 72820 Puebla, Mexico

August 18, 2025

## Abstract

We study the energy dependence of the cross-section for exclusive photoproduction of vector mesons  $J/\psi$  and  $\Upsilon$ , using a solution to the next-to-leading order (NLO) Balitsky-Fadin-Kuraev-Lipatov (BFKL) equation. Our goal is to use BFKL evolution as a benchmark to provide evidence for the presence of non-linear QCD dynamics and signs for the onset of gluon saturation at highest center of mass energies. Our approach determines initial conditions for the proton from the Bartels-Golec Biernat-Kowalski (BGK) dipole model, and evolves the resulting unintegrated gluon distribution using NLO BFKL evolution. For the nucleus, initial conditions are generated through both the impact parameter dependent saturation model (IP-Sat), using a Wood-Saxon distribution and a  $A^{1/3}$  scaling of the saturation scale of the original BGK model. We find that NLO BFKL evolution provides a very good description of the nuclear modification factor for  $J/\psi$  production, if initial conditions are generated through a  $A^{1/3}$  scaled BGK model, while the description fails, if initial conditions are created using the IP-Sat model.

## 1 Introduction

Exclusive photo-production of vector mesons in ultraperipheral collisions at the Large Hadron Collider (LHC) is a very useful process to explore Quantum Chromodynamics (QCD) at ultra-small values of  $x$ . Here,  $x = M_V^2/W^2$ , with  $M_V$  the mass of the vector meson and  $W$  the center of mass energy of the photon-proton or photon-nucleus reaction. The process is primarily of interest for the photoproduction of charmonium, where the charm mass provides a perturbative scale at the boundary to non-perturbative dynamics; it is therefore suitable to potentially observe effects related to the saturation of gluon densities at ultra-low values of  $x$  [1–4]. At low  $x$ , perturbative QCD predicts through the Balitsky-Fadin-Kuraev-Lipatov (BFKL) equation [5–7] a powerlike rise of the gluon distribution. Unitary bounds state however that such a rise cannot continue to arbitrarily small values of  $x$ , but must at some value of  $x$  start to slow down and eventually come to hold. A theoretical framework which predicts such a slow down and saturation of gluon densities are the JIMWLK-BK equations [8–14], which generalize BFKL evolution to the case of high gluon densities.

Photon induced production of charmed vector mesons in exclusive reactions has been extensively explored during the recent years, see e.g. [15–35] for recent theory and [36–39] for

experimental proposals as well as the reviews [40–42]. If data sets collected at both HERA and LHC experiments are combined, such reactions allow to explore low  $x$  dynamics over several orders of magnitude, from  $x \simeq 0.1$  down to  $x = 10^{-6}$ . Exclusive photoproduction on large nuclei is of special interest, since gluon densities are in this case further enhanced through the nuclear mass number  $A$ . Nevertheless, comparison of recently measured ALICE and CMS data for photonuclear production on lead [43, 44] with theory predictions do currently not allow to draw firm conclusions on the possible observation of gluon saturation effects. In particular, descriptions based on a leading twist approach, using nuclear modification factors of parton distribution functions (PDFs), provide currently a competitive description.

A question which one likes to answer in such reactions is whether the observed energy dependence can be explained through an approach which assumes low gluon densities or whether inclusion of high density effects is needed. Predictions which include high density effects are usually based on solutions of non-linear QCD evolution equations, such as the JIMWLK-BK evolution equations. Nevertheless the ability of such schemes to describe data is insufficient to provide evidence for high gluon densities and potentially gluon saturation, since the evolution equations itself are applicable in the low density regime. One therefore needs in addition a framework which assumes low gluon densities and which fails to describe the data set. At first sight, a natural framework for the low density limit is collinear factorization, which provides predictions not only for the low  $x$  region but for all values of  $x$ , while non-perturbative input to Dokshitzer-Gribov-Lipatov-Altarelli-Parisi (DGLAP) evolution equations can be constrained by global fits. While appealing for the aforementioned reasons, relying on collinear factorization only bears the danger to overlook the presence of high gluon densities at low hard scales. DGLAP evolution evolves PDFs from low to high hard scales and testing its validity requires two reactions with a hierarchy of hard scales, i.e. photoproduction of the  $J/\psi$  (low hard scale) and the  $\Upsilon$  (high hard scale). Since  $x = M_V^2/W^2$  and with the maximal center of mass energy  $W$  fixed, bottomonium is limited to larger  $x$  values than charmonium production,  $x_\Upsilon > x_{J/\psi}$ . In addition, predictions at the bottom scale, probe only initial conditions at the charm scale for  $x \geq x_\Upsilon$ . Parametrizations at  $x < x_\Upsilon$  do not enter DGLAP evolution. Predictions at low hard scales and low  $x < x_\Upsilon$ , such as  $J/\psi$  photoproduction, either depend strongly on extrapolation of the parametrization used at larger values of  $x$  or – if  $J/\psi$  data are included in the fit – fit merely the observed  $x$  dependence.

To provide at the very least an alternative framework to test the validity of a low density approach, one may therefore use BFKL evolution to evolve hadronic structure at intermediate  $x \simeq 0.01$  down to low  $x$ . If the BFKL prediction significantly deviates from observation, one can quantify the degree of deviation and therefore arrive at a conclusion to which degree the low density description breaks down. Note that such an approach has been taken before in the literature, see in particular [17, 22, 33]. Unlike [33] we will use in the following NLO BFKL evolution to describe the energy dependence of photoproduction cross-sections, while [17, 22] relied on a fit of the proton impact factor to HERA data and therefore was naturally limited to photoproduction on a proton.

It is needless to say that also this approach is subject to uncertainties: the obtained predictions depend on the transverse momentum distribution of the proton or lead impact factor as well as on the particular choice which one takes to solve the NLO BFKL evolution equations. To constrain the initial transverse momentum distribution for the proton, we will use, unlike in [15, 17, 22], the recently refitted [45] Bartels-Golec Biernat-Kowalski (BGK) model [46] to generate an unintegrated gluon densities at  $x = 0.01$ . For the lead nucleus, we

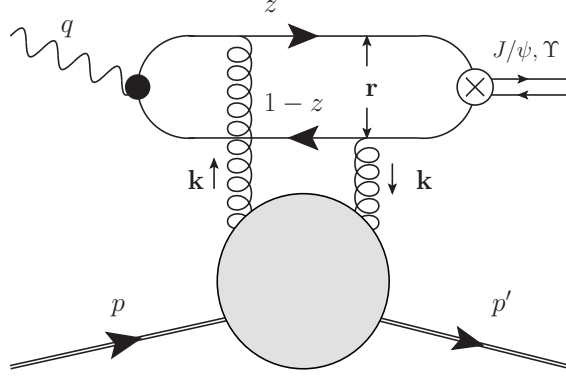


**Figure 1:** Exclusive photoproduction of vector mesons  $J/\psi$  and  $\Upsilon(1s)$ . For the quark-anti quark dipole, we indicate photon momentum fractions  $z$  and  $1-z$  as well as the transverse separation  $\mathbf{r}$ . Finally  $\mathbf{k}$  denotes the transverse momentum transmitted from the unintegrated gluon distribution of the proton or lead nucleus; the latter is indicated through the gray blob;  $\mathbf{r}$  denotes the transverse size of the dipole.

use the impact parameter dependent saturation model [47], based on the BGK model, as well as the BGK model with the effective saturation scale of the model scaled by a factor  $A^{1/3}$ . Our solution of the NLO BFKL equation follows closely the solution of [48, 49], which has been tested both in a fit to HERA data as well as LHC phenomenology [15, 17, 22, 50, 51]. The important difference to these studies is that instead of fitting the initial transverse momentum distribution to data, we will use an already existing dipole model, from which we extract the required impact factor.

To test this setup, we will first explore the proton case, including a comparison to both  $J/\psi$  and  $\Upsilon(1s)$  data. Comparison with the  $\Upsilon$  photoproduction cross-section provides a test in a region of phase space where BFKL evolution is expected to perform well.  $J/\psi$  photoproduction takes on the other hand place at the boundary between perturbative and non-perturbative physics and associated uncertainties are naturally large. Of particular interest is here the study of the nuclear modification factor, since for this quantity uncertainties present in both proton and lead result will cancel to a large extent.

The outline of this paper is as follows: In Sec. 2 we summarize the setup which allows us to obtain the energy dependence of photoproduction cross-sections from the inclusive gluon distribution. We also compare the energy dependence predicted by the BGK model and its nuclear generalizations to data. Sec. 3 discusses the implementation of the solution of the NLO BFKL equation. Sec. 4 contains our results, including a comparison to data. Sec. 5 provides our conclusions.

## 2 Photoproduction cross-sections

We study the process,

$$\gamma(q) + N(p) \rightarrow V(q') + N(p'), \quad V = J/\psi, \Upsilon(1s), N = p, Pb, \quad (1)$$

where  $\gamma$  denotes a quasi-real photon with virtuality  $Q \simeq 0$ .  $W^2 = (q + p)^2$  is the center-of-mass energy squared of the  $\gamma(q) + N(p)$  reaction, see also Fig. 1. With  $t = (q - q')^2$ , the

differential cross-section for the exclusive photo-production of a vector meson can be written as

$$\frac{d\sigma}{dt}(\gamma N \rightarrow VN) = \frac{1}{16\pi} \left| \mathcal{A}_T^{\gamma p \rightarrow Vp}(x, t) \right|^2, \quad V = J/\psi, \Upsilon(1s), \quad (2)$$

with  $\mathcal{A}_T(W^2, t)$  the scattering amplitude for a transverse polarized real photon with color singlet exchange in the  $t$ -channel, where an overall factor  $W^2$  has been already extracted.  $x = M_V^2/W^2$  with  $M_V$  the mass of the vector meson; see also *e.g.* [15]. To access the inclusive gluon distribution, we follow a two-step procedure, frequently employed in the literature: First one determines the differential cross-section at zero momentum transfer  $t = 0$ , which can be related to the inclusive gluon distribution; in a second step one uses the ansatz  $d\sigma/dt \sim \exp[-|t|B_D]$  with the diffractive slope parameter  $B_D$ , which is determined from data. The total cross-section then reads

$$\sigma^{\gamma p \rightarrow Vp}(W^2) = \frac{1}{B_D(W)} \frac{d\sigma}{dt}(\gamma p \rightarrow Vp) \Big|_{t=0}. \quad (3)$$

For photon-proton collisions, we use

$$B_{D,p}^{J/\psi}(W) = \left[ b_{0,p} + 4\alpha'_p \ln \frac{W}{W_0} \right] \text{GeV}^{-2}, \quad (4)$$

where  $W_0 = 90 \text{ GeV}$  and  $b_{0,p}$  and  $\alpha'_p$  have been determined in [52] from a fit to HERA data with  $b_{0,p}^{J/\Psi} = 4.62$ , while  $\alpha'_p{}^{J/\Psi} = 0.171$ . For the  $\Upsilon$  we use  $B_{D,p}^\Upsilon(W) = B_{D,p}^{J/\psi}(W) - b_1 \ln(m_\Upsilon^2/m_{J/\psi}^2)$  [52] with  $b_1 = 0.45 \text{ GeV}^{-2}$  and  $m_\Upsilon = 9.46040 \text{ GeV}$  while  $m_{J/\psi} = 3.096916 \text{ GeV}$ . For photonuclear  $J/\Psi$  production the value  $B_{D,\text{Pb}} = (4.01 \pm 0.15) \cdot 10^2/\text{GeV}^2$  has been determined in [53] from a fit to ALICE data [54], which we will also use for  $\Upsilon$  photoproduction. The subleading real part of the scattering amplitude can be finally estimated from the imaginary part using

$$\frac{\text{Re}\mathcal{A}(x)}{\text{Im}\mathcal{A}(x)} = \tan \frac{\lambda(x)\pi}{2}, \quad \lambda(x) = \frac{d \ln \text{Im}\mathcal{A}(x)}{d \ln 1/x}. \quad (5)$$

As noted in [15], the dependence of the slope parameter  $\lambda$  on  $x$  provides a sizable correction to the  $W$  dependence of the complete cross-section. We therefore do not assume  $\lambda = \text{const.}$ , but determine the slope  $\lambda$  directly from the  $x$ -dependent imaginary part of the scattering amplitude.

## 2.1 Wave function overlap

Within high energy factorization, the imaginary part of the scattering amplitude at  $t = 0$  is obtained as a convolution of the light-front wave function overlap and the dipole cross-section. Using a simple boosted Gaussian model for the vector meson wave function, based on the Brodsky-Huang-Lepage prescription [55–57], we have

$$\text{Im}\mathcal{A}_T^{\gamma p \rightarrow Vp}(x, t = 0) = \int d^2\mathbf{r} \int_0^1 \frac{dz}{4\pi} (\Psi_V^* \Psi_T)(r, z) \sigma_{q\bar{q}}(x, r), \quad (6)$$

t

**Table 1:** Parameters of the boosted Gaussian vector meson wave functions for  $J/\Psi$  [59] and  $\Upsilon(1s)$  [60].

Meson	$m_f/\text{GeV}$	$\mathcal{N}_T$	$\mathcal{R}^2/\text{GeV}^{-2}$	$M_V/\text{GeV}$
$J/\Psi$	$m_c = 1.4$	0.57	2.45	3.097
$\Upsilon(1s)$	$m_b = 4.2$	0.481	0.57	9.460

where  $r = |\mathbf{r}|$  denotes the transverse separation of the dipole and [58]

$$(\Psi_V^* \Psi_T) = \frac{\hat{e}_f e N_c}{\pi z(1-z)} \left\{ m_f^2 K_0(m_f r) \phi_T(r, z) - [z^2 + (1-z)^2] m_f K_1(m_f r) \partial_r \phi_T(r, z) \right\}, \quad (7)$$

with

$$\phi_T^{1s}(r, z) = \mathcal{N}_{T,1s} z(1-z) \exp \left( -\frac{m_f^2 \mathcal{R}_{1s}^2}{8z(1-z)} - \frac{2z(1-z)r^2}{\mathcal{R}_{1s}^2} + \frac{m_f^2 \mathcal{R}_{1s}^2}{2} \right). \quad (8)$$

The free parameters of Eq. (8) have been determined in various studies from the normalization and orthogonality of the wave functions as well as the decay width of the vector mesons. In the following we use the values found in [59, 60] which we summarize in Tab. 1.

## 2.2 Dipole cross-sections

A simple model for the dipole cross-section is provided by the Bartels, Golec-Biernat, Kowalski (BGK) model [46],

$$\sigma_{q\bar{q}}^{\text{BGK}}(x, r) = \sigma_0^{\text{BGK}} \left[ 1 - \exp \left( -\frac{r^2 \pi^2 \alpha_s(\mu_r^2) x g(x, \mu_r^2)}{3\sigma_0^{\text{BGK}}} \right) \right], \quad (9)$$

which is obtained through exponentiating the collinear dipole cross-section [46, 61]. The model has been recently refitted [45] for dipole scattering on a proton to combined HERA data. The collinear gluon distribution  $g(x, \mu^2)$  is subject to a leading order DGLAP evolution equation without quarks,

$$\frac{d}{d\mu^2} g(x, \mu^2) = \frac{\alpha_s}{2\pi} \int_x^1 \frac{dz}{z} P_{gg}(z) g(x/z, \mu^2), \quad xg(x, Q_0^2) = A_g x^{-\lambda_g} (1-x)^{5.6}, \quad (10)$$

where  $xg(x, Q_0^2)$  denotes the gluon distribution at the initial scale  $Q_0 = 1$  GeV. Following [45], we evaluate the gluon distribution and the QCD running coupling at the dipole size dependent scale

$$\mu_r^2 = \frac{\mu_0^2}{1 - \exp(-\mu_0^2 r^2 / C)}. \quad (11)$$

The remaining parameters of the model have been obtained as  $\sigma_0^{\text{BGK}} = (22.93 \pm 0.27)$  mb,  $A_g = 1.07 \pm 0.13$ ,  $\lambda_g = 0.11 \pm 0.03$ ,  $C = 0.27 \pm 0.04$ ,  $\mu_0^2 = (1.74 \pm 0.16)$  GeV<sup>2</sup>. To arrive at a suitable generalization of the BGK model for dipole scattering on a large nucleus, we consider

two options: the impact parameter dependent saturation (IPSat) model and a description where the effective saturation scale  $Q_s^2(x)$  is scaled by a factor  $A^{\frac{1}{3}}$  with  $A$  the number of nucleons in the nucleus. The formulation of the IPSat model is based on the optical Glauber model. Using a Wood Saxon distribution, one averages over the position of different nucleons and finds [47, 62]

$$\frac{d\sigma_{q\bar{q}}^{\text{IPSat}}}{d^2b} = 2 \left[ 1 - \left( 1 - \frac{1}{2} T_A(b) \sigma_{q\bar{q}}(x, r) \right)^A \right], \quad (12)$$

with nuclear thickness function  $T(b)$  and Wood-Saxon distribution  $\rho^{\text{WS}}(r)$  given by

$$T(b) = \int_{-\infty}^{\infty} dz \rho^{\text{WS}}(\sqrt{z^2 + b^2}), \quad \rho^{\text{WS}}(r) = \frac{\mathcal{N}^{\text{WS}}}{1 + e^{\frac{r - R_{\text{Pb}}}{d}}}; \quad (13)$$

$\mathcal{N}^{\text{WS}}$  is fixed through  $\int d^3r \rho^{\text{WS}}(r) = 1$ . For the following study we will employ the values obtained in [63],  $R_{\text{Pb}} = 6.624$  fm and  $d = 0.549$  fm which have been also used in [64]. As an alternative to the IPSat model, we consider the scenario where the dipole no longer scatters on individual nucleons, but on the Lorentz contracted nucleus as a whole. Within high energy factorization, the exchanged  $t$ -channel gluons have delta-like support and it is therefore natural to assume scattering on a Lorentz contracted large nucleus, which gives rise to  $A^{1/3}$  scaling of the saturation scale. To include such a scaling within the BGK model we use

$$\sigma_{q\bar{q}}^{A^{\frac{1}{3}}}(x, r) = \sigma_0^{\text{Pb}} \left[ 1 - \exp \left( - \frac{r^2 \pi^2 \alpha_s(\mu_r^2) A^{\frac{1}{3}} x g(x, \mu_r^2)}{3 \sigma_0^{\text{BGK}}} \right) \right]. \quad (14)$$

Based on simple geometric considerations, see also [53], one expects the parameter  $\sigma_0^{\text{Pb}}$  to scale approximately as  $\sim A^{2/3}$ . In practice, such a simple rescaling yields still a considerable off-set in the overall normalization. We therefore determine  $\sigma_0^{\text{Pb}}$  from a fit to combined ALICE-CMS data set as  $\sigma_0^{\text{Pb}} = (1.587 \pm 0.008)$  barn. Comparing to simple scaling we find that  $\sigma_0^{\text{Pb}}/(\sigma_0 \cdot 208^{2/3}) \simeq 1.97$ , while the obtained value is approximately 0.63 times the maximal value of  $\sigma_{q\bar{q}}^{\text{IPSat}}(x, r \rightarrow \infty)$ .

The energy dependence predicted by these dipoles models, including a comparison to data is shown in Fig. 2 and Fig. 3. Since we are mainly interested in the energy dependence, we allow for adjustments in the overall normalization, through introducing a parameter  $N$  through  $\Im \mathcal{M} \rightarrow N \cdot \Im \mathcal{M}$ , which we adjust through a fit to  $J/\psi$  data for  $W < 500$  GeV. While we find a very good description of the energy dependence of the  $J/\psi$  photoproduction cross-section on a proton, Fig. 2, for  $W < 500$  GeV, the model undershoots proton data for  $W > 500$  GeV. For the  $\Upsilon(1s)$  photoproduction cross-section we use the normalization determined from the  $J/\psi$  fit. We observe that both energy dependence and normalization is well described in this case. As a side note we mention that our own earlier attempts used instead of the BGK model the GBW model; while the energy dependence is still well described for the  $\Upsilon$ , one finds a considerable offset in normalization, if the latter is fixed using  $J/\psi$  data. Comparison of the photo-nuclear cross-section with data is shown in Fig. 3. While the IPSat model provides a good estimate of the overall normalization of the cross-section, which for the  $A^{\frac{1}{3}}$  scaled BGK model has been fitted to data, its energy dependence is in

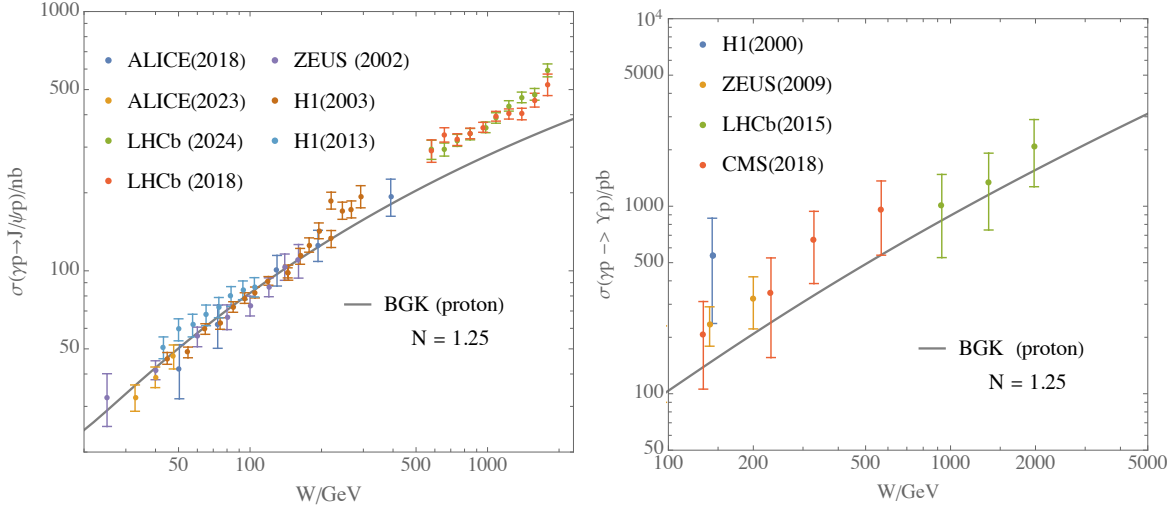


**Figure 2:** Energy dependence of the total cross-sections for exclusive photoproduction of  $J/\Psi$  (left) and  $\Upsilon(1s)$  on a proton, using the BGK dipole model. We further display photo-production data for  $J/\psi$  from ZEUS [65] [66], H1 [67, 68] [69, 70], ALICE [71, 72] and LHCb [73, 74] as well as  $\Upsilon(1s)$  data obtained at H1 [75], ZEUS [76], LHCb [77] and CMS [78].

general too strong and does not agree with data. Even with the proton dipole cross-section undershooting data, the IP-Sat model – which has been obtained from the proton dipole cross-section – overshoots data. The  $A^{1/3}$  scaled BGK model provides on the other hand a good description of the energy dependence, in particular if one ignores the off-set with high energy CMS data. Even though the observation is merely made on the levels of saturation models, our results seems to indicate that assuming scattering of the dipole on individual nucleons is no longer justified. Treating the lead nucleus as a scaled-up proton provides on the other hand a more accurate description of the energy dependence. We further present the nuclear suppression factor which is defined as  $S_{\text{Pb}} = \sqrt{\sigma_{\gamma\text{Pb}}/\sigma_{\gamma\text{Pb}}^{\text{IA}}}$ . Following [43, 79] the cross-section in the impulse approximation  $\sigma_{\gamma\text{Pb}}^{\text{IA}}$  is obtained as

$$\sigma_{\gamma\text{Pb}}^{\text{IA}} = \frac{d\sigma_{\gamma p \rightarrow J/\psi p}}{dt} \Big|_{t=0} \cdot \int_{|t|_{\min}}^{\infty} d|t| |F(t)|^2, \quad F(t) = 208 \cdot \int d^3r e^{i\vec{q} \cdot \vec{r}} \rho^{\text{WS}}(r), \quad (15)$$

with  $t = -\vec{q}^2$  and  $t_{\min} \simeq 0$  for LHC kinematics. As expected, the IP-Sat model does not describe the energy dependence of the nuclear modification factor. The  $A^{1/3}$  scaled BGK model provides on the other hand a good description of data, even though it overshoots high energy CMS data points.

### 3 Energy dependence through BFKL

In the following the above dipole models are used to generate initial conditions for BFKL evolution.

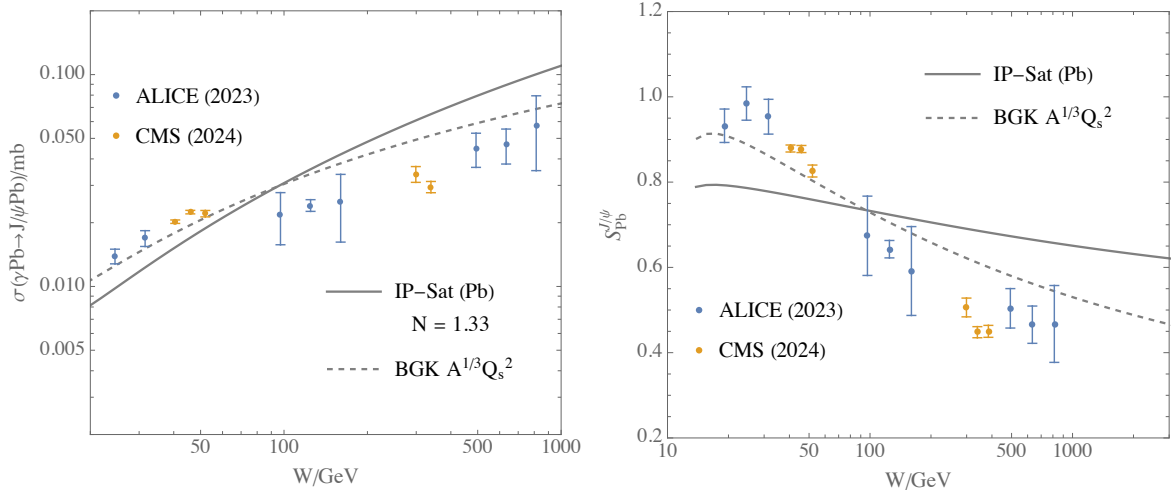


**Figure 3:** Energy dependence of the  $J/\psi$  photoproduction cross-section on lead (left) and the nuclear modification factor (right) obtained from the dipole models Eq. (12) and Eq. (14). We further show ALICE [43] and CMS [44] data.

### 3.1 BFKL evolution of dipole cross-sections

Our starting point is the following factorization of the elastic scattering amplitude in the forward limit  $t = 0$ ,

$$\Im \mathcal{M}_T^{\gamma p \rightarrow V p}(x, 0) = \int dk^2 \int dq^2 \Phi^{\gamma V}(k) \mathcal{F}_{\text{BFKL}}^{\text{DIS}}\left(\frac{x_0}{x}, k, q\right) G(x_0, q), \quad (16)$$

where  $\mathcal{F}_{\text{BFKL}}^{\text{DIS}}$  denotes the NLO BFKL Green's function in the DIS scheme and

$$\Phi^{\gamma V}(k, m_f) = \frac{4\pi^2}{N_c} \int d^2\mathbf{r} \int_0^1 \frac{dz}{4\pi} \frac{1 - e^{i\mathbf{k}\cdot\mathbf{r}}}{\mathbf{k}^2} (\Psi_V^* \Psi_T)(r, z), \quad (17)$$

provides the impact factor for the photon vector meson transition.  $G(x_0, q)$  denotes on the other hand the unintegrated gluon distribution at  $x_0 = 0.01$ . The expression can be constructed as follows: at leading order, one has the following relation between dipole cross-section and unintegrated gluon distribution  $G(x, k)$ ,

$$\sigma_{q\bar{q}}(x, r) = \frac{4\pi^2\alpha_s}{N_c} \int \frac{d^2\mathbf{k}}{\pi} \frac{1 - e^{i\mathbf{k}\cdot\mathbf{r}}}{\mathbf{k}^2} G(x, k), \quad k = |\mathbf{k}|, \quad (18)$$

To evolve  $G(x_0, k)$  to low  $x$ , we use a solution of the NLO BFKL Green's function elaborated in [48–50]

$$G(x, k) = \int_0^\infty \frac{dq^2}{q^2} \mathcal{F}_{\text{BFKL}}^{\text{DIS}}\left(\frac{x_0}{x}, k, q\right) G(x_0, q). \quad (19)$$

The unintegrated gluon distribution at  $x_0$  can be finally determined from the dipole cross-section using<sup>1</sup>,

$$G(x_0, k) = \frac{N_c k^2}{8\pi^2\alpha_s} \int_0^\infty dr r J_0(rk) [\sigma_0 - \sigma_{q\bar{q}}(x_0, r)], \quad \sigma_0 = \lim_{r \rightarrow \infty} \sigma_{q\bar{q}}(x_0, r). \quad (20)$$

<sup>1</sup>See [80] for a compact summary of the procedure



Eq. (19) describes correctly the low  $x$  evolution of the unintegrated gluon distribution if high density corrections are suppressed by powers of the strong coupling  $\alpha_s$ , *i.e.* if the gluon distribution does not saturate the bound  $G \sim 1/\alpha_s$ . This is the central hypothesis of this section: we assume that such corrections are irrelevant and we explore to which extent this leads to tension with data. We further note that both Eq. (18),(20) depend on  $\alpha_s$ , while the dependence cancels, if both expressions are combined. In general it is not clear whether both strong couplings are to be evaluated at the same scale, which gives rise to a normalization ambiguity, see also the discussion in [80].

To solve NLO BFKL evolution, we follow closely [48, 49]. In transverse Mellin space we have

$$\mathcal{F}_{\text{BFKL}}^{\text{DIS}}\left(\frac{x_0}{x}, k, q\right) = \frac{1}{k^2} \int_{\frac{1}{2}-i\infty}^{\frac{1}{2}+i\infty} \frac{d\gamma}{2\pi i} (k^2)^{\gamma-1} \hat{f}\left(\frac{x_0}{x}, \frac{M^2}{Q_s^2(x_0)}, \frac{\overline{M}^2}{M^2}, \gamma\right) (q^2)^{-\gamma}, \quad (21)$$

with  $\hat{f}$  an operator in  $\gamma$  space and defined as

$$\hat{f} = \left(\frac{1}{x}\right)^{\chi(\gamma, \mu, M)} \cdot \left\{ 1 - \frac{\bar{\alpha}_s^2 \beta_0}{8N_c} \log\left(\frac{x_0}{x}\right) \left[ \overleftarrow{\partial}_\gamma \chi_0(\gamma) - \chi_0(\gamma) \overrightarrow{\partial}_\gamma - 2\chi_0(\gamma) \ln M^2 \right] \right\}, \quad (22)$$

see also the related discussion in [15, 50, 81, 82]. Here  $\bar{\alpha}_s = \alpha_s(\mu)N_c/\pi$ , while  $\mu$  denotes the renormalization scale.  $M$  is on the other hand a parameter which has been introduced to identify the central value of the renormalization scale of the problem; it cancels to NLO accuracy. In the following, we first determine a suitable choice for  $M$  and then vary  $\mu$  in the range  $M/2, 2M$  to estimate the uncertainty associated with our prediction. The determination of  $M$  will be discussed below.  $\chi(\gamma, \mu, M)$  is the next-to-leading logarithmic (NLL) BFKL kernel after collinear improvements; in addition large terms proportional to the first coefficient of the QCD beta function,  $\beta_0 = 11N_c/3 - 2n_f/3$  are resummed through employing a Brodsky-Lepage-Mackenzie (BLM) optimal scale setting scheme [83]. For those details we follow very closely the treatment in [15, 48, 49]. The NLL kernel with collinear improvements reads

$$\begin{aligned} \chi(\gamma, \mu, M) = & \bar{\alpha}_s \chi_0(\gamma) + \bar{\alpha}_s^2 \tilde{\chi}_1(\gamma) - \frac{1}{2} \bar{\alpha}_s^2 \chi_0'(\gamma) \chi_0(\gamma) \\ & + \chi_{RG}(\bar{\alpha}_s, \gamma, \tilde{a}, \tilde{b}) - \frac{\bar{\alpha}_s^2 \beta_0}{4N_c} \chi_0(\gamma) \log \frac{\mu^2}{M^2}, \end{aligned} \quad (23)$$

with the leading-order BFKL eigenvalue,

$$\chi_0(\gamma) = 2\psi(1) - \psi(\gamma) - \psi(1-\gamma). \quad (24)$$

Employing BLM optimal scale setting and the momentum space (MOM) physical renormalization scheme based on a symmetric triple gluon vertex with  $Y \simeq 2.343907$  and gauge

parameter  $\xi = 3$  one obtains the following next-to-leading order BFKL eigenvalue

$$\begin{aligned}\tilde{\chi}_1(\gamma) = & \tilde{\mathcal{S}}\chi_0(\gamma) + \frac{3}{2}\zeta(3) + \frac{\Psi''(\gamma) + \Psi''(1-\gamma) - \phi(\gamma) - \phi(1-\gamma)}{4} \\ & - \frac{\pi^2 \cos(\pi\gamma)}{4 \sin^2(\pi\gamma)(1-2\gamma)} \left[ 3 + \left(1 + \frac{n_f}{N_c^3}\right) \frac{2+3\gamma(1-\gamma)}{(3-2\gamma)(1+2\gamma)} \right] \\ & + \frac{1}{8} \left[ \frac{3}{2}(Y-1)\xi + \left(1 - \frac{Y}{3}\right)\xi^2 + \frac{17Y}{2} - \frac{\xi^3}{6} \right] \chi_0(\gamma),\end{aligned}\quad (25)$$

where  $\tilde{\mathcal{S}} = 1/3 - \pi^2/12$ . We note that the specific choice on scheme and parameters follows the one of [48, 84], see also the discussion in [85]. Within this scheme one then replaces  $\bar{\alpha}_s \rightarrow \tilde{\alpha}_s(\gamma)$  with

$$\tilde{\alpha}_s(\bar{\alpha}_s, \gamma) = \frac{\bar{\alpha}_s(\mu)}{1 + \frac{\bar{\alpha}_s \beta_0}{4N_c} \left[ \frac{1}{2}\chi_0(\gamma) - \frac{5}{3} + 2\left(1 + \frac{2}{3}Y\right) \right]}, \quad (26)$$

which yields the effective running coupling constant to be used for the Green's function. For the numerical study we use the NLO QCD running coupling with  $\alpha_s(M_Z) = 0.1181$  and  $M_Z = 91.1876$  GeV. The term which achieves a resummation of collinear enhanced terms in the NLO BFKL kernel reads

$$\begin{aligned}\chi_{RG}(\bar{\alpha}_s, \gamma, a, b) = & \bar{\alpha}_s(1 + a\bar{\alpha}_s)(\psi(\gamma) - \psi(\gamma - b\bar{\alpha}_s)) - \frac{\bar{\alpha}_s^2}{2}\psi''(1-\gamma) - \frac{b\bar{\alpha}_s^2 \cdot \pi^2}{\sin^2(\pi\gamma)} \\ & + \frac{1}{2} \sum_{m=0}^{\infty} \left( \gamma - 1 - m + b\bar{\alpha}_s - \frac{2\bar{\alpha}_s(1 + a\bar{\alpha}_s)}{1 - \gamma + m} \right. \\ & \left. + \sqrt{(\gamma - 1 - m + b\bar{\alpha}_s)^2 + 4\bar{\alpha}_s(1 + a\bar{\alpha}_s)} \right).\end{aligned}\quad (27)$$

For details on the derivation of this term we refer to the discussion in [48]. The coefficients  $\tilde{a}, \tilde{b}$  which enter the collinear resummation term Eq. (27) are obtained as the coefficients of the  $1/\gamma$  and  $1/\gamma^2$  poles of the NLO eigenvalue. We have

$$\begin{aligned}\tilde{a} = & -\frac{13}{36} \frac{n_f}{N_c^3} - \frac{55}{36} + \frac{3Y-3}{16}\xi + \frac{3-Y}{24}\xi^2 - \frac{1}{48}\xi^3 + \frac{17}{16}Y, \\ \tilde{b} = & -\frac{n_f}{6N_c^3} - \frac{11}{12}.\end{aligned}\quad (28)$$

With the elements of Eq. (22) fixed, we determine as a next step the Mellin transform of  $\Phi^{\gamma V}$  and  $G(x_0, q)$ . We have [15]

$$\begin{aligned}\phi^{\gamma V}(\gamma, m_f) = & \int_0^\infty \frac{dk^2}{k^2} \left( \frac{k^2}{m_f^2} \right)^\gamma \Phi^{\gamma V}(k, m_f) = \int_0^1 \frac{dz}{4\pi} \tilde{\phi}_{V,T}(\gamma, z, m_f) \\ \tilde{\phi}_{V,T}(\gamma, z, m_f) = & e\hat{e}_f 8\pi^2 \mathcal{N}_T \frac{\Gamma(\gamma)\Gamma(1-\gamma)}{m_f^2} \left( \frac{m_f^2 \mathcal{R}^2}{8z(1-z)} \right)^{2-\gamma} e^{-\frac{m_f^2 \mathcal{R}^2}{8z(1-z)}} e^{\frac{m_f^2 \mathcal{R}^2}{2}}, \\ & \left[ U\left(2-\gamma, 1, \frac{m_f^2 \mathcal{R}^2}{8z(1-z)}\right) + [z^2 + (1-z)^2] \frac{\Gamma(3-\gamma)}{\Gamma(2-\gamma)} U\left(3-\gamma, 2, \frac{m_f^2 \mathcal{R}^2}{8z(1-z)}\right) \right],\end{aligned}\quad (29)$$

where  $U(a, b, z)$  is a hypergeometric function of the second kind or Kummer's function<sup>2</sup>. We note that normalization of the above impact factor is inversely proportional to the heavy quark mass; its precise value takes therefore an important role in fixing the normalization of the photoproduction cross-section. While the heavy quark mass is the natural scale of the impact factor describing the photon-vector meson transition, the choice is less clear for the hadronic impact factor. While one might use as a first guess the saturation scale of the dipole model at initial  $x_0 = 0.01$ , the NLO BFKL fit to HERA data of [48, 49] suggests to use a smaller value, of the order of a few hundred MeV. Within the current setup, we then define for each unintegrated gluon distribution at  $x_0 = 0.01$  a characteristic scale  $Q_0$  through

$$1 - \sigma_{q\bar{q}}(x_0, r = 1/Q_0)/\sigma_0 = e^{-1}; \quad (30)$$

the resulting scale  $Q_0$  is then half the saturation scale of a corresponding GBW type model [45]. Note that the above choice only affects our result in the way we fix the scale  $M$ . We then finally arrive at

$$\phi^{\text{ugd}}(\gamma, Q_0) = \int_0^\infty dq^2 \left( \frac{q^2}{Q_0^2} \right)^{-\gamma} G^{\text{ugd}}(x_0, q, Q_0). \quad (31)$$

To determine this quantity, we first determine numerically  $G^{\text{ugd}}(x_0)$  from the dipole cross-section and then from the resulting expression  $\phi^{\text{ugd}}(\gamma)$ . With these ingredients we have

$$\begin{aligned} \Im \mathcal{A}(x, 0) = N \int_{\frac{1}{2}-i\infty}^{\frac{1}{2}+i\infty} \frac{d\gamma}{2\pi i} \left( \frac{m_f^2}{Q_0^2} \right)^\gamma \left( \frac{x_0}{x} \right)^{\chi(\gamma, \mu, M)} \phi^{\gamma V}(\gamma, m_f) \phi^{\text{ugd}}(\gamma, Q_0) \\ \cdot \left\{ 1 - \frac{\tilde{\alpha}_s^2(\tilde{\alpha}_s, \gamma) \beta_0 \chi_0(\gamma)}{8N_c} \log \left( \frac{x_0}{x} \right) \cdot \left[ \frac{d}{d\gamma} \ln \frac{\phi^{\gamma V}(\gamma, m_f)}{\phi^{\text{ugd}}(\gamma, Q_0)} - 2 \ln \frac{M^2}{m_f Q_0} \right] \right\}, \quad (32) \end{aligned}$$

where  $N$  is a factor that collects the various sources of normalization uncertainty. While  $N = \mathcal{O}(1)$ , its precise value will be fixed by a comparison to data. We finally set  $M^2 = k \cdot m_f \cdot Q_0$  with  $k$  a parameter which we vary. While  $k = 1$  is the natural choice, we will explore also other values in the following; recall that the value of  $M$  sets the central value for the renormalization scale  $\mu$ , which we vary in addition in the range  $[M/2, 2M]$ .

### 3.2 Instability of the NLO solution

The above solution to the NLO BFKL equation possesses an instability for ultra-low values of  $x$ , see also the discussion in [17, 22]: for sufficiently small values of  $k$ , the second term in the second line of Eq. (32) is negative and growing in magnitude with diminishing  $x$ . Unlike [17, 22], which employed directly the results of the HSS fit, the effect can be avoided in the current case through choosing sufficiently large value of  $k$ . Such a choice comes however at an undesired cost: the growth with energy of the resulting photo-production is too strong and does not agree with data. We only find agreement with data for a negative NLO correction. Since we would like to explore the degree to which BFKL evolution can be adapted to still

---

<sup>2</sup>With respect to the expression found in [15], we corrected an incorrect power of  $m_f$  in the exponent as well as relative factor of 2 between the first and the second term

describe photoproduction data, we allow in the following for values of  $k$  which yield such a contribution. At the same time, we demand that the BFKL prediction is still well justified within QCD perturbation theory. We define to this end two criteria, which our solution must fulfill. We first define

$$\Im\mathcal{A}(x, 0) = \Im\mathcal{A}^{(0)}(x, 0) + \Im\mathcal{A}^{(1)}(x, 0), \quad (33)$$

where

$$\begin{aligned} \Im\mathcal{A}^{(0)}(x, 0) &= N \int_{\frac{1}{2}-i\infty}^{\frac{1}{2}+i\infty} \frac{d\gamma}{2\pi i} \left( \frac{m_f^2}{Q_0^2} \right)^\gamma \left( \frac{x_0}{x} \right)^{\chi(\gamma, \mu, M)} \phi^{\gamma V}(\gamma, m_f) \phi^{\text{ugd}}(\gamma, Q_0), \\ \Im\mathcal{A}^{(1)}(x, 0) &= N \int_{\frac{1}{2}-i\infty}^{\frac{1}{2}+i\infty} \frac{d\gamma}{2\pi i} \left( \frac{m_f^2}{Q_0^2} \right)^\gamma \left( \frac{x_0}{x} \right)^{\chi(\gamma, \mu, M)} \phi^{\gamma V}(\gamma, m_f) \phi^{\text{ugd}}(\gamma, Q_0) \\ &\quad \cdot \left\{ -\frac{\tilde{\alpha}_s^2(\tilde{\alpha}_s, \gamma) \beta_0 \chi_0(\gamma)}{8N_c} \log\left(\frac{x_0}{x}\right) \cdot \left[ \frac{d}{d\gamma} \ln \frac{\phi^{\gamma V}(\gamma, m_f)}{\phi^{\text{ugd}}(\gamma, Q_s^2(x_0))} - 2 \ln k \right] \right\}, \end{aligned} \quad (34)$$

see also the discussion in [17]. Given these expressions we can define now 2 criteria which indicate that the choice of  $k$  is no longer natural and stability of the perturbative description is to be lost:

- First we require that  $|\Im\mathcal{A}^{(1)}(x^{\min}, 0)|/\Im\mathcal{A}^{(0)}(x^{\min}, 0) < 0.5$  at the lowest observed value of  $x$ ; for the proton  $x_p^{\min} \simeq 3.0 \cdot 10^{-6}$ , whereas for lead one currently has  $x_{Pb}^{\min} \simeq 1.45 \cdot 10^{-5}$ .
- A second criteria is that we require a positive slope of the scattering amplitude  $\lambda > 0$ , i.e.  $\Im\mathcal{A}(x^{\min}, 0)$  must still grow with energy.

For  $J/\psi$  photo-production, these criteria allow to push the BFKL prediction to the limits of its applicability. Photoproduction of the  $\Upsilon$  provides on the other hand an important cross-check since one expects a stable perturbative prediction in this case.

## 4 Results and discussion

As a first step, we provide predictions for the energy dependence of the photoproduction on the proton, both for  $J/\psi$  and  $\Upsilon$  vector mesons. Condition Eq. (30) yields in this case  $Q_0^{\text{prot.}} = 0.256$  GeV, which is numerically very close to the scale of the impact factor found in [48, 49]. Our results are shown in Fig. 4. We would like to stress that even for the proton case, the ability of NLO BFKL evolution to describe the energy dependence of photoproduction is a non-trivial observation. The initial conditions for the unintegrated gluon distribution were not fitted to collider data, employing NLO BFKL evolution as the underlying evolution equation. Instead, the initial conditions have been obtained from the BGK dipole model, which itself has been fitted to inclusive DIS data. The fact that NLO BFKL evolution provides a good description of the energy dependence of both the  $J/\psi$  and  $\Upsilon$  photoproduction cross-section is yet another confirmation that NLO BFKL is in general terms a useful framework

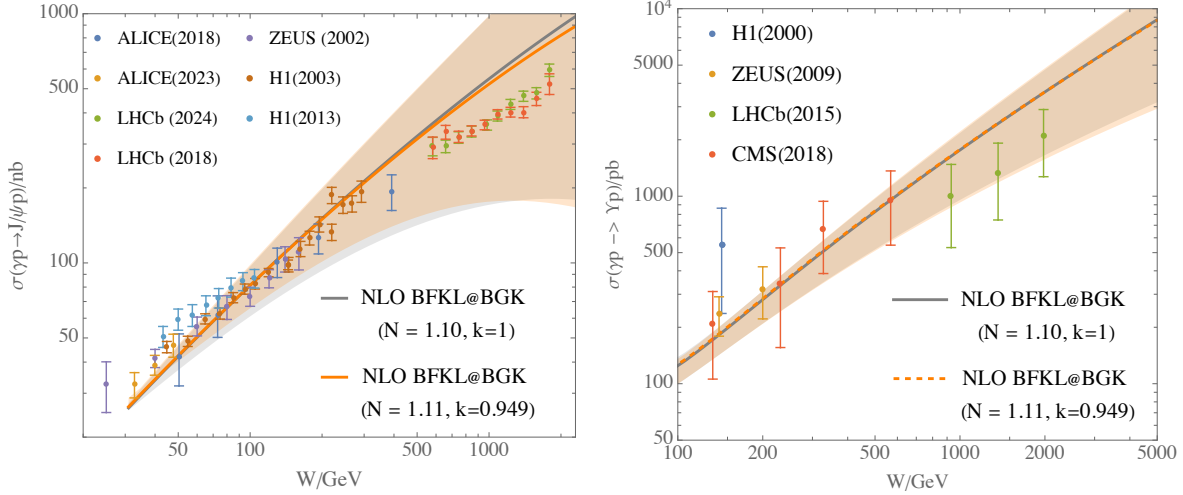


**Figure 4:** Energy dependence of the  $J/\psi$  (left) and  $\Upsilon$  (right) photoproduction cross-section as obtained from acting with the NLO BFKL Green's function on the BGK dipole cross-section at  $x_0 = 0.01$ . We displayed the same data sets as in Fig. 2

to predict the energy dependence of perturbative QCD cross-sections. We both study the scenario of  $k = 1$  as well as of minimal  $k = 0.949$ . The deviation of the overall normalization constant is very close to one and has been fixed through a fit to  $J/\psi$  data at  $W < 500$  GeV. The central values of the BFKL prediction overshoot in both cases data points at  $W > 500$  GeV. An improved description with a smaller value of  $k$ , would however violate our stability conditions, formulated in Sec. 3.2. The uncertainty of the  $J/\psi$  prediction at  $W > 500$  GeV is nevertheless already considerable. While this is unpleasant, such a behavior was to be expected, based on the results of [17, 22]. As argued there, the BFKL prediction leaves certain space for non-linear QCD evolution – which in some cases can provide an improved description – but the uncertainties are too large to provide definite evidence. Uncertainties are considerably reduced for  $\Upsilon$  photoproduction. Last but not least we would like to comment that one may also try to obtain the dipole distribution function using the conceptually simpler Golec-Biernat Wüsthof (GBW) dipole model. While this model has the advantage that analytic expressions can be obtained for the Mellin transform of the unintegrated gluon distribution, it lacks corrections due to DGLAP evolution at the initial  $x_0$ , which gives rise to a certain off-set in normalization between the  $J/\psi$  and  $\Upsilon$  photoproduction cross-section. While not central to the objective of this paper, we believe that this is an interesting observation since it indicates that DGLAP type corrections are also needed for impact factors.

BFKL evolution for  $J/\psi$  photoproduction on lead is shown in Fig. 5, including a comparison to data. For the IP-Sat model we find  $Q_0^{\text{IPs}} = 0.344$  GeV, which is only marginally larger than the proton results. For the  $A^{\frac{1}{3}}$  scaled proton saturation scale, we have instead  $Q_0^{A^{\frac{1}{3}}} = 0.622$  GeV. As for the proton, we show predictions both for the case  $k = 1$  and for the minimal  $k$  value, which is allowed by the stability requirements of Sec. 3.2. While the higher values of  $Q_0$  allow to extend the prescription down to lower values of  $k$ , the impact on the energy dependence is rather small. For the determination of the normalization, we exclude data points with  $W > 280$  GeV. The resulting adjustments in normalization are larger than in the case of the proton. We note that not fixing the normalization leads to an improved

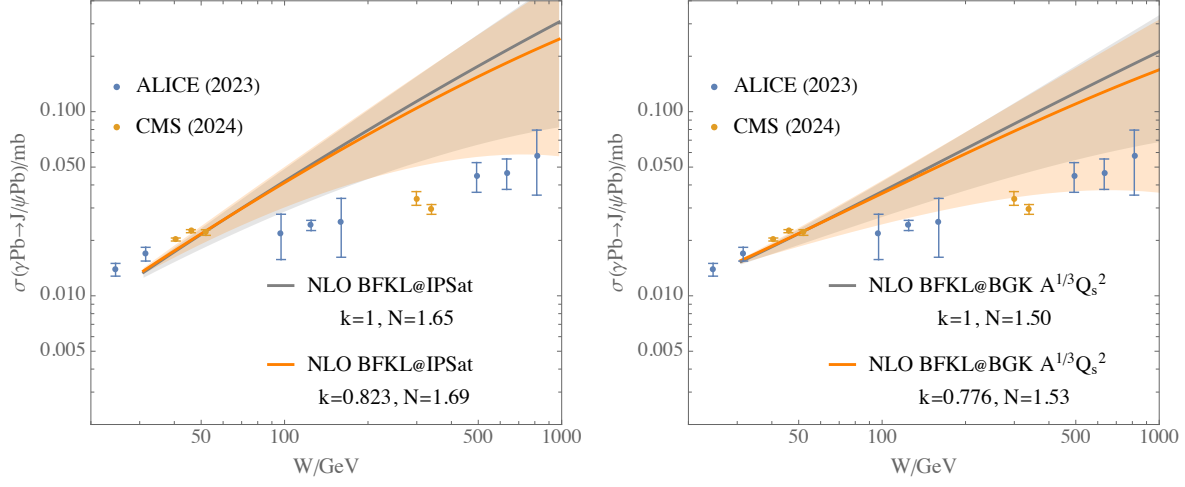


**Figure 5:** Energy dependence of the  $J/\psi$  photoproduction cross-section as obtained from acting with the NLO BFKL Green's function on the IP-Sat (left) and  $A^{1/3}$  scaled BGK dipole cross-section at  $x_0 = 0.01$ . We displayed the same data sets as in Fig. 3

description of values at  $W > 280$  GeV, while one clearly misses the low energy data points. Since our main goal is to study predictions for the energy dependence, fixing the low energy normalization appears to be the right choice here. If initial conditions for BFKL evolution

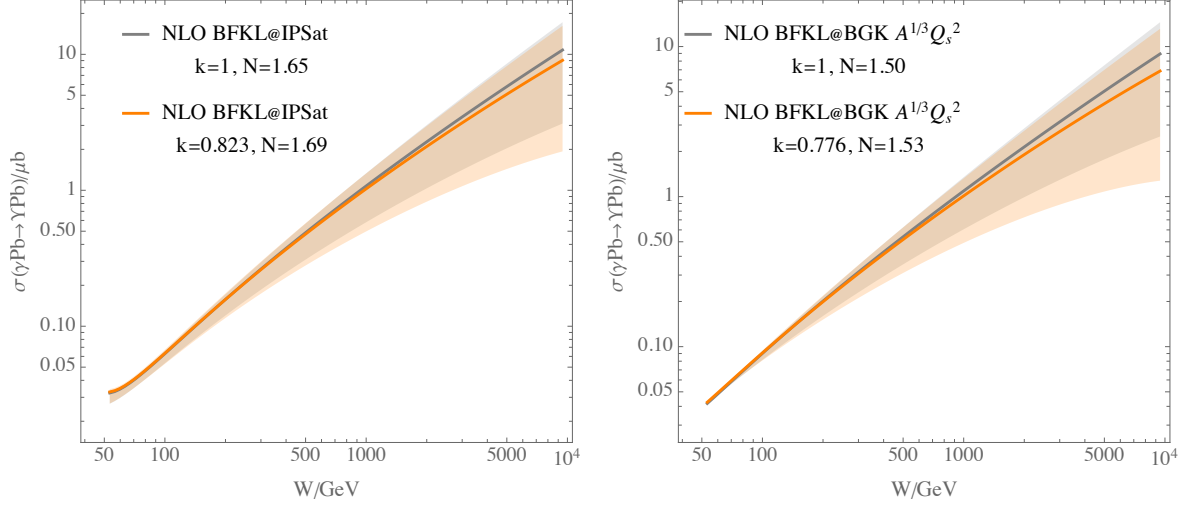


**Figure 6:** Energy dependence of the  $\Upsilon$  photoproduction cross-section as obtained from acting with the NLO BFKL Green's function on the IP-Sat (left) and  $A^{1/3}$  scaled BGK dipole cross-section at  $x_0 = 0.01$ .

are generated through the IPSat model, we find strong tension between the obtained energy dependence and data. Assuming that the IP-Sat model provides the correct description of the dipole cross-section at values of  $x > 0.01$ , we can exclude almost with certainty that the energy dependence of photonuclear  $J/\psi$  production is described by low density QCD low  $x$  evolution. While the  $A^{1/3}$  scaled BGK model also provides a BFKL prediction which clearly

overshoots data, the situation is less clear in that case. In particular for  $k = 0.776$ , the majority of data points is still described within the large uncertainty of the BFKL prediction. At the same time, one needs to keep in mind that the description is based on a significantly increased value of  $Q_0$ , which requires strong correlations between individual nucleons in the lead nucleus.

In Fig. 6 we finally provide predictions for  $\Upsilon$  photonuclear production. As in the proton case, uncertainties are reduced for the  $\Upsilon$  due to the higher hard scale. Similar to the  $J/\psi$  case we find that BFKL based on IPSat initial conditions grows stronger with energy than the  $A^{1/3}$  scaled BGK saturation model.

In Fig. 7 we finally provide the nuclear modification factor for both  $J/\psi$  and  $\Upsilon$  photonuclear production. As for saturation models we determine the nuclear modification factor as

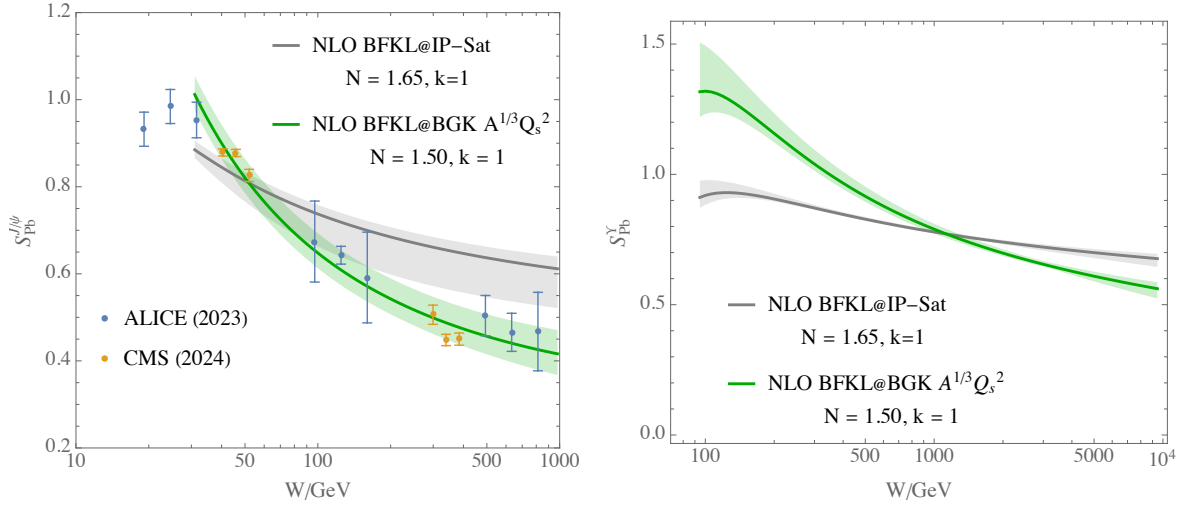


**Figure 7:** Nuclear modification factor for  $J/\psi$  (left) and  $\Upsilon$  (right). We further show ALICE [43] and CMS [44] data.

$S_{\gamma\text{Pb}} = \sqrt{\sigma_{\gamma\text{Pb}}/\sigma_{\gamma\text{Pb}}^{\text{IA}}}$ , where  $\sigma_{\gamma\text{Pb}}^{\text{IA}}$  is determined from Eq. (15), using now the proton cross-section with BFKL evolution. As one might expect, the theoretical uncertainties associated with BFKL evolution reduce significantly for the nuclear modification factor  $S_{\gamma\text{Pb}}^{J/\psi}$ . While the energy dependence predicted by the NLO BFKL evolution with IPSat model initial conditions is within uncertainties in agreement with ALICE data, it clearly overshoots CMS data points at high  $W$ . The description based on NLO BFKL evolution based on  $A^{1/3}$  scaled BGK model describes the energy dependence of the nuclear modification factor very well, over the entire range in energies. For photonuclear production of  $\Upsilon(1s)$ , the nuclear modification factor is within our framework significantly reduced, albeit the deviation from one is still sizable at highest values of  $W$ .

## 5 Conclusions

We explored to which extend NLO BFKL evolution is able to describe the energy dependence of photoproduction cross-sections of vector mesons  $J/\psi$  and  $\Upsilon(1s)$  on a proton and on a lead nucleus. Unlike previous studies, e.g. [33], which provided a solution of the BFKL

equation for non-zero momentum transfer  $t \neq 0$ , but were restricted to leading order in the perturbative expansion, our solution is restricted to  $t = 0$ , while the complete NLO corrections have been included, together with a resummation of collinear enhanced terms in the NLO BFKL Green's function. As a first result we find that we need to push the NLO BFKL description to the limits of its applicability to describe the observed energy dependence. To guarantee perturbative stability, we defined two criteria, i.e. a limit on the size of a perturbative correction to the Green's function as well as a positive slope at smallest observed  $x$  values. With these criteria we find that for  $J/\psi$  photoproduction, central values of the BFKL description overshoot both proton and lead data. While proton data agree with the BFKL description within the sizable theory uncertainties, lead data only agree with the BFKL prediction within uncertainties, if the  $A^{\frac{1}{3}}$  scaled BGK model is used to generate initial conditions for BFKL evolution. The photoproduction cross-section of the  $\Upsilon$  on the proton is on the other hand very well described. A particularly interesting observable is provided by the nuclear modification factor: we find that the sizable uncertainties of the BFKL description reduces significantly in this case and we find an excellent description of data for initial conditions created by the  $A^{\frac{1}{3}}$  scaled BGK model, whereas BFKL evolution based on the IPSat model clearly overshoots data.

Our result indicate the following: at first there are strong indications that the gluon density per transverse area scales as  $A^{\frac{1}{3}}$  for the lead nucleus. The  $A^{\frac{1}{3}}$  scaled dipole model provides itself a good description of the photonuclear cross-section as well as of the nuclear modification factor. At the same time, the  $A^{\frac{1}{3}}$  scaled dipole model provides adequate initial conditions for NLO BFKL evolution. This is particularly remarkable since descriptions based on the IPSat model fails. Our result for the nuclear modification factor seems furthermore to indicate that a description of the energy dependence does currently not require the inclusion of non-linear terms into low  $x$  evolution. Nevertheless one should keep in mind that the NLO BFKL description is only possible due to the negative perturbative correction to the NLO BFKL Green's function. Choosing the renormalization scale in a way such that this term is very small or positive, a description of the energy dependence would be not possible. In this sense, our result cannot exclude completely the need of a non-linear terms in the evolution (which arguably would have a similar effect). However our results seem to imply that the size of non-linear terms should be of similar magnitude for both photoproduction on the proton and a lead nucleus.

For future studies it would be interesting to generate initial conditions for NLO BFKL evolution directly from nuclear PDFs. While this is challenging, it would probably reduce further the uncertainty in fixing initial conditions. A future measurement of the  $\Upsilon$  production at lead targets would be of great use to further verify the current approach. While one expects non-linear dynamics to further weaken in this case, different initial conditions to NLO BFKL evolution provide significantly different results for the nuclear modification factor in the case of the  $\Upsilon$ ; its measurement would therefore clearly contribute to clarify the situation further and to fix the correct initial conditions. Finally, measurement of the dependence of the vector meson production cross-section on photon virtuality at the future EIC, would allow determine the lead impact factor from a fit to EIC data and therefore reduce uncertainties.



## Acknowledgments

We acknowledge support by IANN-QCD network and discussions with Zhoudunming Tu. MH is grateful to the BNL EIC Theory institute for financial support and to Krzysztof Kutak and members of the BNL nuclear theory group for useful discussions.

## References

- [1] L.V. Gribov, E.M. Levin, and M.G. Ryskin. Semihard Processes in QCD. *Phys. Rept.*, 100:1–150, 1983.
- [2] Astrid Morreale and Farid Salazar. Mining for Gluon Saturation at Colliders. *Universe*, 7(8):312, 2021, 2108.08254.
- [3] Martin Hentschinski et al. White Paper on Forward Physics, BFKL, Saturation Physics and Diffraction. *Acta Phys. Polon. B*, 54(3):3–A2, 2023, 2203.08129.
- [4] A. C. Aguilar et al. Latin American Strategy Forum for Research Infrastructure (III LASF4RI Contribution): The glue that binds us all - Latin America and the Electron-Ion Collider. *Braz. J. Phys.*, 55(4):145, 2025, 2409.18407.
- [5] E.A. Kuraev, L.N. Lipatov, and Victor S. Fadin. The Pomeranchuk Singularity in Nonabelian Gauge Theories. *Sov. Phys. JETP*, 45:199–204, 1977.
- [6] E. A. Kuraev, L. N. Lipatov, and Victor S. Fadin. Multi - Reggeon Processes in the Yang-Mills Theory. *Sov. Phys. JETP*, 44:443–450, 1976.
- [7] I.I. Balitsky and L.N. Lipatov. The Pomeranchuk Singularity in Quantum Chromodynamics. *Sov. J. Nucl. Phys.*, 28:822–829, 1978.
- [8] I. Balitsky. Operator expansion for high-energy scattering. *Nucl. Phys. B*, 463:99–160, 1996, hep-ph/9509348.
- [9] Jamal Jalilian-Marian, Alex Kovner, and Heribert Weigert. The Wilson renormalization group for low x physics: Gluon evolution at finite parton density. *Phys. Rev. D*, 59:014015, 1998, hep-ph/9709432.
- [10] Yuri V. Kovchegov. Small x F(2) structure function of a nucleus including multiple pomeron exchanges. *Phys. Rev. D*, 60:034008, 1999, hep-ph/9901281.
- [11] Edmond Iancu, Andrei Leonidov, and Larry D. McLerran. Nonlinear gluon evolution in the color glass condensate. 1. *Nucl. Phys. A*, 692:583–645, 2001, hep-ph/0011241.
- [12] Heribert Weigert. Unitarity at small Bjorken x. *Nucl. Phys. A*, 703:823–860, 2002, hep-ph/0004044.
- [13] Edmond Iancu, Andrei Leonidov, and Larry D. McLerran. The Renormalization group equation for the color glass condensate. *Phys. Lett. B*, 510:133–144, 2001, hep-ph/0102009.

- [14] Elena Ferreiro, Edmond Iancu, Andrei Leonidov, and Larry McLerran. Nonlinear gluon evolution in the color glass condensate. 2. *Nucl. Phys. A*, 703:489–538, 2002, hep-ph/0109115.
- [15] I. Bautista, A. Fernandez Tellez, and Martin Hentschinski. BFKL evolution and the growth with energy of exclusive  $J/\psi$  and  $\Upsilon$  photoproduction cross sections. *Phys. Rev. D*, 94(5):054002, 2016, 1607.05203.
- [16] J. Cepila, J.G. Contreras, and M. Matas. Collinearly improved kernel suppresses Coulomb tails in the impact-parameter dependent Balitsky-Kovchegov evolution. *Phys. Rev. D*, 99(5):051502, 2019, 1812.02548.
- [17] A. Arroyo Garcia, M. Hentschinski, and K. Kutak. QCD evolution based evidence for the onset of gluon saturation in exclusive photo-production of vector mesons. *Phys. Lett. B*, 795:569–575, 2019, 1904.04394.
- [18] M. Krelina, V. P. Goncalves, and J. Cepila. Coherent and incoherent vector meson electroproduction in the future electron-ion colliders: the hot-spot predictions. *Nucl. Phys. A*, 989:187–200, 2019, 1905.06759.
- [19] Spencer R. Klein and Heikki Mäntysaari. Imaging the nucleus with high-energy photons. *Nature Rev. Phys.*, 1(11):662–674, 2019, 1910.10858.
- [20] B. Z. Kopeliovich, M. Krelina, J. Nemchik, and I. K. Potashnikova. Ultraperipheral nuclear collisions as a source of heavy quarkonia. *Phys. Rev. D*, 107(5):054005, 2023, 2008.05116.
- [21] D. Bendova, J. Cepila, J. G. Contreras, and M. Matas. Photonuclear  $J/\psi$  production at the LHC: Proton-based versus nuclear dipole scattering amplitudes. *Phys. Lett. B*, 817:136306, 2021, 2006.12980.
- [22] Martin Hentschinski and Emilio Padrón Molina. Exclusive  $J/\Psi$  and  $\Psi(2s)$  photo-production as a probe of QCD low  $x$  evolution equations. *Phys. Rev. D*, 103(7):074008, 2021, 2011.02640.
- [23] Laszlo Jenkovszky, Vladyslav Libov, and Magno V. T. Machado. The reggeometric pomeron and exclusive production of  $J/\psi$  and  $\psi(2S)$  in ultraperipheral collisions at the LHC. *Phys. Lett. B*, 824:136836, 2022, 2111.13389.
- [24] Christopher Alexander Flett. *Exclusive Observables to NLO and Low  $x$  PDF Phenomenology at the LHC*. PhD thesis, U. Liverpool (main), U. Liverpool (main), 2021.
- [25] Heikki Mäntysaari and Jani Penttala. Exclusive heavy vector meson production at next-to-leading order in the dipole picture. *Phys. Lett. B*, 823:136723, 2021, 2104.02349.
- [26] Heikki Mäntysaari and Jani Penttala. Complete calculation of exclusive heavy vector meson production at next-to-leading order in the dipole picture. *JHEP*, 08:247, 2022, 2204.14031.

- [27] Victor P. Goncalves, Bruno D. Moreira, and Luana Santana. Exclusive  $\rho$  and  $J/\Psi$  photoproduction in ultraperipheral pO and OO collisions at energies available at the CERN Large Hadron Collider. *Phys. Rev. C*, 107(5):055205, 2023, 2210.11911.
- [28] Xiao-Yun Wang, Fancong Zeng, and Quanjin Wang. Systematic analysis of the proton mass radius based on photoproduction of vector charmoniums. *Phys. Rev. D*, 105(9):096033, 2022, 2204.07294.
- [29] Heikki Mäntysaari, Farid Salazar, and Björn Schenke. Energy dependent nuclear suppression from gluon saturation in exclusive vector meson production. *Phys. Rev. D*, 109(7):L071504, 2024, 2312.04194.
- [30] Jan Cepila, Jesus Guillermo Contreras, Marek Matas, and Alexandra Ridzikova. Incoherent  $J/\psi$  production at large  $-\mathbf{t}$ — identifies the onset of saturation at the LHC. *Phys. Lett. B*, 852:138613, 2024, 2312.11320.
- [31] Heikki Mäntysaari, Jani Penttala, Farid Salazar, and Björn Schenke. Finite-size effects on small- $x$  evolution and saturation in proton and nuclear targets. *Phys. Rev. D*, 111(5):054033, 2025, 2411.13533.
- [32] J. Cepila, J. G. Contreras, M. Matas, and M. Vaculciak. Impact-parameter-dependent solutions to the Balitsky-Kovchegov equation at next-to-leading order. *Phys. Rev. D*, 111(9):096015, 2025, 2412.08571.
- [33] Jani Penttala and Christophe Royon. Gluon saturation effects in exclusive heavy vector meson photoproduction. *Phys. Lett. B*, 864:139394, 2025, 2411.14815.
- [34] J. Cepila, J. G. Contreras, and M. Vaculciak. Exclusive quarkonium photoproduction: Predictions with the Balitsky-Kovchegov equation including the full impact-parameter dependence. *Phys. Rev. D*, 111(5):056002, 2025, 2501.09462.
- [35] J. Nemchik and J. Óbertová. Searching for gluon saturation effects in momentum transfer dependence of coherent charmonium electroproduction off nuclei. 7 2025, 2507.01531.
- [36] Spencer Klein et al. New opportunities at the photon energy frontier. 9 2020, 2009.03838.
- [37] Alexander Bylinkin, Joakim Nystrand, and Daniel Tapia Takaki. Vector meson photoproduction in UPCs with FoCal. 11 2022, 2211.16107.
- [38] Physics of the ALICE Forward Calorimeter upgrade. 2023.
- [39] Pedro E. A. da Costa, André V. Giannini, Victor P. Goncalves, and Bruno D. Moreira. Photoproduction of heavy vector mesons in peripheral  $PbPb$  collisions at the Large Hadron Collider. 5 2025, 2505.14019.
- [40] S. Amoroso et al. Snowmass 2021 Whitepaper: Proton Structure at the Precision Frontier. *Acta Phys. Polon. B*, 53(12):12–A1, 2022, 2203.13923.
- [41] L. Frankfurt, V. Guzey, A. Stasto, and M. Strikman. Selected topics in diffraction with protons and nuclei: past, present, and future. *Rept. Prog. Phys.*, 85(12):126301, 2022, 2203.12289.

- [42] F. Arleo et al. Nuclear Cold QCD: Review and Future Strategy. 6 2025, 2506.17454.
- [43] Shreyasi Acharya et al. Energy dependence of coherent photonuclear production of  $J/\psi$  mesons in ultra-peripheral Pb-Pb collisions at  $\sqrt{s_{NN}}=5.02$  TeV. 5 2023, 2305.19060.
- [44] Armen Tumasyan et al. Probing Small Bjorken- $x$  Nuclear Gluonic Structure via Coherent  $J/\psi$  Photoproduction in Ultraperipheral Pb-Pb Collisions at  $s_{NN}=5.02$  TeV. *Phys. Rev. Lett.*, 131(26):262301, 2023, 2303.16984.
- [45] Krzysztof Golec-Biernat and Sebastian Sapeta. Saturation model of DIS : an update. *JHEP*, 03:102, 2018, 1711.11360.
- [46] J. Bartels, Krzysztof J. Golec-Biernat, and H. Kowalski. A modification of the saturation model: DGLAP evolution. *Phys. Rev. D*, 66:014001, 2002, hep-ph/0203258.
- [47] Henri Kowalski and Derek Teaney. An Impact parameter dipole saturation model. *Phys. Rev. D*, 68:114005, 2003, hep-ph/0304189.
- [48] Martin Hentschinski, Agustín Sabio Vera, and Clara Salas. Hard to Soft Pomeron Transition in Small- $x$  Deep Inelastic Scattering Data Using Optimal Renormalization. *Phys. Rev. Lett.*, 110(4):041601, 2013, 1209.1353.
- [49] Martin Hentschinski, Agustín Sabio Vera, and Clara Salas.  $F_2$  and  $F_L$  at small  $x$  using a collinearly improved BFKL resummation. *Phys. Rev. D*, 87(7):076005, 2013, 1301.5283.
- [50] Grigorios Chachamis, Michal Deák, Martin Hentschinski, Germán Rodrigo, and Agustín Sabio Vera. Single bottom quark production in  $k_\perp$ -factorisation. *JHEP*, 09:123, 2015, 1507.05778.
- [51] F.G. Celiberto, D. Gordo Gómez, and A. Sabio Vera. Forward Drell–Yan production at the LHC in the BFKL formalism with collinear corrections. *Phys. Lett. B*, 786:201–206, 2018, 1808.09511.
- [52] Jan Cepila, Jan Nemchik, Michal Krelina, and Roman Pasechnik. Theoretical uncertainties in exclusive electroproduction of S-wave heavy quarkonia. *Eur. Phys. J. C*, 79(6):495, 2019, 1901.02664.
- [53] Marco Alcazar Peredo and Martin Hentschinski. Ratio of  $J/\Psi$  and  $\Psi(2s)$  exclusive photoproduction cross sections as an indicator for the presence of nonlinear QCD evolution. *Phys. Rev. D*, 109(1):014032, 2024, 2308.15430.
- [54] Shreyasi Acharya et al. First measurement of the  $—t—$ dependence of coherent  $J/\psi$  photonuclear production. *Phys. Lett. B*, 817:136280, 2021, 2101.04623.
- [55] Stanley J. Brodsky, Tao Huang, and G.Peter Lepage. The Hadronic Wave Function in Quantum Chromodynamics. 6 1980.
- [56] B.E. Cox, J.R. Forshaw, and R. Sandapen. Diffractive upsilon production at the LHC. *JHEP*, 06:034, 2009, 0905.0102.

- [57] J. Nemchik, Nikolai N. Nikolaev, and B.G. Zakharov. Scanning the BFKL pomeron in elastic production of vector mesons at HERA. *Phys. Lett. B*, 341:228–237, 1994, hep-ph/9405355.
- [58] H. Kowalski, L. Motyka, and G. Watt. Exclusive diffractive processes at HERA within the dipole picture. *Phys. Rev. D*, 74:074016, 2006, hep-ph/0606272.
- [59] Néstor Armesto and Amir H. Rezaeian. Exclusive vector meson production at high energies and gluon saturation. *Phys. Rev. D*, 90(5):054003, 2014, 1402.4831.
- [60] V. P. Gonçalves, B. D. Moreira, and F. S. Navarra. Exclusive  $\Upsilon$  photoproduction in hadronic collisions at CERN LHC energies. *Phys. Lett. B*, 742:172–177, 2015, 1408.1344.
- [61] L. Frankfurt, A. Radyushkin, and M. Strikman. Interaction of small size wave packet with hadron target. *Phys. Rev. D*, 55:98–104, 1997, hep-ph/9610274.
- [62] Heikki Mäntysaari and Pia Zurita. In depth analysis of the combined HERA data in the dipole models with and without saturation. *Phys. Rev. D*, 98:036002, 2018, 1804.05311.
- [63] H. De Vries, C. W. De Jager, and C. De Vries. Nuclear charge and magnetization density distribution parameters from elastic electron scattering. *Atom. Data Nucl. Data Tabl.*, 36:495–536, 1987.
- [64] Jan Cepila and Marek Matas. Contribution of the non-linear term in the Balitsky–Kovchegov equation to the nuclear structure functions. *Eur. Phys. J. A*, 56(9):232, 2020, 2006.16136.
- [65] S. Chekanov et al. Exclusive photoproduction of  $J/\psi$  mesons at HERA. *Eur. Phys. J. C*, 24:345–360, 2002, hep-ex/0201043.
- [66] S. Chekanov et al. Exclusive electroproduction of  $J/\psi$  mesons at HERA. *Nucl. Phys. B*, 695:3–37, 2004, hep-ex/0404008.
- [67] A. Aktas et al. Elastic  $J/\psi$  production at HERA. *Eur. Phys. J. C*, 46:585–603, 2006, hep-ex/0510016.
- [68] C. Alexa et al. Elastic and Proton-Dissociative Photoproduction of  $J/\psi$  Mesons at HERA. *Eur. Phys. J. C*, 73(6):2466, 2013, 1304.5162.
- [69] C. Alexa et al. Elastic and Proton-Dissociative Photoproduction of  $J/\psi$  Mesons at HERA. *Eur. Phys. J. C*, 73(6):2466, 2013, 1304.5162.
- [70] A. Aktas et al. Elastic  $J/\psi$  production at HERA. *Eur. Phys. J. C*, 46:585–603, 2006, hep-ex/0510016.
- [71] Shreyasi Acharya et al. Energy dependence of exclusive  $J/\psi$  photoproduction off protons in ultra-peripheral p–Pb collisions at  $\sqrt{s_{NN}} = 5.02$  TeV. *Eur. Phys. J. C*, 79(5):402, 2019, 1809.03235.
- [72] Shreyasi Acharya et al. Exclusive and dissociative  $J/\psi$  photoproduction, and exclusive dimuon production, in p–Pb collisions at  $s_{NN}=8.16$  TeV. *Phys. Rev. D*, 108(11):112004, 2023, 2304.12403.

- [73] Roel Aaij et al. Central exclusive production of  $J/\psi$  and  $\psi(2S)$  mesons in  $pp$  collisions at  $\sqrt{s} = 13$  TeV. *JHEP*, 10:167, 2018, 1806.04079.
- [74] Roel Aaij et al. Measurement of exclusive  $J/\psi$  and  $\psi(2S)$  production at  $\sqrt{s} = 13$  TeV. *SciPost Phys.*, 18(2):071, 2025, 2409.03496.
- [75] C. Adloff et al. Elastic photoproduction of  $J/\psi$  and Upsilon mesons at HERA. *Phys. Lett. B*, 483:23–35, 2000, hep-ex/0003020.
- [76] S. Chekanov et al. Exclusive photoproduction of Upsilon mesons at HERA. *Phys. Lett. B*, 680:4–12, 2009, 0903.4205.
- [77] Roel Aaij et al. Measurement of the exclusive  $\Upsilon$  production cross-section in  $pp$  collisions at  $\sqrt{s} = 7$  TeV and 8 TeV. *JHEP*, 09:084, 2015, 1505.08139.
- [78] Albert M. Sirunyan et al. Measurement of exclusive  $\Upsilon$  photoproduction from protons in pPb collisions at  $\sqrt{s_{NN}} = 5.02$  TeV. *Eur. Phys. J. C*, 79(3):277, 2019, 1809.11080. [Erratum: Eur.Phys.J.C 82, 343 (2022)].
- [79] V. Guzey, E. Kryshen, M. Strikman, and M. Zhalov. Evidence for nuclear gluon shadowing from the ALICE measurements of PbPb ultraperipheral exclusive  $J/\psi$  production. *Phys. Lett. B*, 726:290–295, 2013, 1305.1724.
- [80] Agnieszka Łuszczak, Marta Łuszczak, and Wolfgang Schäfer. Unintegrated gluon distributions from the color dipole cross section in the BGK saturation model. *Phys. Lett. B*, 835:137582, 2022, 2210.02877.
- [81] Agustin Sabio Vera. The Effect of NLO conformal spins in azimuthal angle decorrelation of jet pairs. *Nucl. Phys. B*, 746:1–14, 2006, hep-ph/0602250.
- [82] Agustin Sabio Vera and Florian Schwennsen. The Azimuthal decorrelation of jets widely separated in rapidity as a test of the BFKL kernel. *Nucl. Phys. B*, 776:170–186, 2007, hep-ph/0702158.
- [83] Stanley J. Brodsky, G.Peter Lepage, and Paul B. Mackenzie. On the Elimination of Scale Ambiguities in Perturbative Quantum Chromodynamics. *Phys. Rev. D*, 28:228, 1983.
- [84] Stanley J. Brodsky, Victor S. Fadin, Victor T. Kim, Lev N. Lipatov, and Grigori B. Pivovarov. High-energy QCD asymptotics of photon-photon collisions. *JETP Lett.*, 76:249–252, 2002, hep-ph/0207297.
- [85] Francesco Giovanni Celiberto and Michael Fucilla. Diffractive semi-hard production of a  $J/\psi$  or a  $\Upsilon$  from single-parton fragmentation plus a jet in hybrid factorization. *Eur. Phys. J. C*, 82(10):929, 2022, 2202.12227.